DALTON

On the electronic structures and spectra of $NiCl_2$ and $CuCl_2$

Adam J. Bridgeman

University Chemical Laboratories, Lensfield Road, Cambridge CB2 1EW, UK

The geometry and ground state of $NiCl_2$ have been studied using local density-functional (LDF) calculations within the linear combination of Gaussian-type orbitals (LCGTO) framework. The molecule is found to be linear with a $^3\Sigma_g^-$ ground state in agreement with recent experimental results but contrary to previous theoretical studies. The calculated bond length and vibrational frequencies are in excellent agreement with experiment. A cellular ligand-field (CLF) analysis of the spectrum has been performed. The LDF and CLF calculations provide a consistent description of the bonding and suggest that the chloride ions are acting as good σ and π donors in this molecule with both roles enhanced compared to systems with higher co-ordination numbers. A proper account of the important interaction of the d_σ orbital with the antibonding σ_g^+ orbital is given using a cylindrically symmetric 'void' cell. A recent CLF analysis of $CuCl_2$ is shown to be incorrect because of the treatment of the void interaction. A new study of the ligand-field spectrum of $CuCl_2$ is presented, the results of which are consistent with the LDF and CLF studies on $NiCl_2$ and with recent molecular orbital and LDF calculations on $CuCl_2$.

The geometry and electronic structure of the apparently simple transition-metal dihalides provoke continuous interest and debate. Two of the most extensively studied of these systems are $NiCl_2$ and $CuCl_2$. Qualitative crystal-field arguments and simple molecular orbital considerations suggest that the d orbitals in linear transition-metal dihalides are split into three levels, σ_g^+, π_g and δ_g, with relative energies $d_\sigma > d_\pi > d_\delta$. The stimulus for the present work was provided by recent experimental measurements of the electronic spectra of these molecules and the theoretical studies of $CuCl_2$ which both predict that the ground states are derived from a reversal of the energies of d_σ and d_π. In this study the ground state of $NiCl_2$ is investigated using density-functional theory (DFT). The ground state is found to agree with that suggested by experiment. This ground state necessitates a reassignment of the ligand-field spectrum of this molecule and this has been carefully implemented within the cellular ligand-field (CLF) model. The ground state and ligand-field spectrum of $CuCl_2$ have been the subject of three recent theoretical studies.[1–3] All of these predict the unexpected ground state $^2\Pi_g$, derived from the orbital configuration $\delta_g^4\sigma_g^{+1}\pi_g^4$. There was no agreement, however, on the assignment of the ligand-field spectrum. Along with a DFT study of this molecule, Deeth[2] reported CLF calculations suggesting a discrepancy between the two descriptions of the relative σ to π bonding ratio. This analysis is shown to be flawed. A new CLF study suggests an assignment of the spectrum in agreement with the results of recent experiments and the coupled-pair functional Hartree–Fock (CPF-HF) calculations of Bauschlicher and Roos.[1]

Earlier Studies

$NiCl_2$

The study of isolated molecules like $NiCl_2$ presents considerable challenges both to the spectroscopist and to the theoretical chemist. The compounds have to be studied experimentally either in cryogenic matrices or in the gas phase. The matrix work leads to sharp spectra but rotational information is lost and there is always the possibility that the matrix can affect the geometry of the guest molecule. This is likely to be a problem for low-co-ordination molecules such as these because of the rather low energy barrier to distortion. In a nitrogen matrix, for example, $NiCl_2$ appears to be strongly bent with a bond angle of around 130° and to have quite short Ni–N distances,[4] whereas in an argon matrix[5] it is probably linear.[6]

The gas-phase electronic spectrum[7–9] of $NiCl_2$ contains the following features: (*i*) a weak and broad absorption in the region 4000–8000 cm^{-1}; (*ii*) weak absorption around 10 000 cm^{-1}; (*iii*) a very sharp peak at 11 700 cm^{-1}, probably due to a spin-forbidden transition; the width of the peak strongly suggests that this band is due to a 'spin-flip' transition; (*iv*) a relatively intense peak at *ca.* 13 000 cm^{-1}, probably due to a spin-allowed transition; (*v*) a series of weak features at *ca.* 14 000, 16 000 and 18 000 cm^{-1}; and (*vi*) a relatively intense peak at *ca.* 21 700 cm^{-1}, probably due to a spin-allowed transition. Gas-phase studies require high temperatures to generate sufficient material to study. At such temperatures many rotational and vibrational levels are populated and this leads to complicated spectra. The large amplitude of the soft bending mode also makes the interpretation of electron diffraction patterns difficult. In recent years, however, techniques have been developed[10] to cool the gas-phase sample and so obtain considerably simplified spectra.

In a key series of papers[11–13] the band at 21 700 cm^{-1} (460 nm) has been studied at increasingly low temperatures. With the d orbitals split as expected from simple crystal-field considerations, only a $^3\Pi_g$ ($\delta_g^4\pi_g^3\sigma_g^{+1}$) or $^3\Delta_g$ ($\delta_g^3\pi_g^4\sigma_g^{+1}$) ground state seems likely,[14] although the diamagnetic, low-spin, $^1\Sigma_g^+$ ($\delta_g^4\pi_g^4$) ground state has also been considered.[15,16] In all previous theoretical studies[7,9,14–19] the ground state has been predicted to be $^3\Pi_g$. The band at around 460 nm ($\approx$21 700 cm^{-1}) in the absorption spectrum is predicted by the ligand-field calculations of Lever and Hollebone,[14] DeKock and Gruen[8,9] and by Smith[17] to be due to the $^3\Sigma_g^-$ (P) ⟵ $^3\Pi_g$ (F) transition. A triplet splitting pattern in the band at 460 nm was observed by Grieman *et al.*[11] This splitting was constant throughout the vibronic bands and the same isotope splitting was observed in each of the components. Grieman *et al.* show that this indicates that the same vibronic levels are involved in each of the constituents of the triplet and that the observations are consistent with the assignment of the ground state as a spin triplet and the splitting to be due to spin–orbit coupling. The observed splittings among the three components, labelled F_1, F_2 and F_3, were found to be 95.9 ($F_1 - F_2$) and 149.1 cm^{-1} ($F_2 - F_3$). DeKock and Gruen[9] calculated the spin–orbit splitting between the adjacent levels of the inverted $^3\Pi_g$ ground state to be 106 ($^3\Pi_{g2} - {}^3\Pi_{g1}$), 134 ($^3\Pi_{g1} - {}^3\Pi_{g0^+}$) and 586

cm^{-1} ($^3\Pi_{g0+} - {}^3\Pi_{g0-}$). The triplet splitting observed in the spectrum was thus tentatively assigned to the spin–orbit splitting of the $^3\Pi_g$ ground state.

In a later study, Ashworth *et al.*[12] recorded the same spectrum at lower temperature. For the assignment suggested above, depopulation of the higher spin–orbit levels of the ground state would lead to lower intensity in both the F_2 and F_3 features. However, only the intensity of F_3 is reduced on cooling. Ashworth *et al.* thus suggest that F_1 and F_2 arise from transitions from the lowest spin–orbit level of the ground state to adjacent levels in the excited state; F_3 is then assigned to the transition from the lower level of the ground state to the upper level of the excited state. This proposition is supported by the observation in this spectrum of a fourth component, assigned by Ashworth *et al.* to the transition between the upper level of the ground state to the upper level of the excited state and by rotational analysis of the band.[13] The spin–orbit splitting of the ground state into two levels implied by this spectrum is not consistent with a $^3\Pi_g$ ground state and Ashworth *et al.* showed that the experimental results suggest that the ground state is $^3\Sigma_g^-$.

$CuCl_2$

The gas-phase spectrum[7,8] consists of a ('IR') band at *ca.* 9000 cm^{-1} and a considerably more intense ('Red') band at *ca.* 19 000 cm^{-1}. No electronic spectrum has been reported below 4000 cm^{-1}. Before the CPF-HF calculations of Bauschlicher and Roos[1] all theoretical investigations[7,8,14,17–22] predicted a $^2\Sigma_g^+$ ($\delta_g^4\pi_g^4\sigma_g^{+1}$) ground state but differed according to the assignment of the two observed transitions. Interest in this system was rekindled by the calculations of Bauschlicher and Roos and by the possible use of $CuCl_2$ as a chemically generated laser system. The calculations predicted a $^2\Pi_g$ ($\Omega = \frac{1}{2}$) ground state arising from a $\delta_g^4\pi_g^3\sigma_g^{+2}$ configuration. The ligand-field transitions are calculated to occur at *ca.* 1600 ($^2\Sigma_g^-$, $\Omega = \frac{1}{2}$), *ca.* 7500 ($^2\Delta_g$, $\Omega = \frac{5}{2}$) and at *ca.* 9700 cm^{-1} ($^2\Delta_g$, $\Omega = \frac{3}{2}$). The Red band is assigned to a charge-transfer transition. The spectrum has received considerable recent experimental attention. These studies have involved observation of the emission[23–26] or laser-induced fluorescence.[27,28] These are all consistent with a $^2\Pi_g$ ground state. The emission spectrum, for example, shows a doublet splitting assigned to the transition to the two spin–orbit components ($\Omega = \frac{1}{2}, \frac{3}{2}$) of the ground state.

There have also been two recent local density functional (LDF) studies of this molecule. Deeth[2] has performed LDF Slater-type orbital (STO) calculations on each of the ligand-field states. Rogemond *et al.*[3] have reported LDF calculations in the linear combination of Gaussian-type orbitals (LCGTO) approach for all the low-lying electronic states. Both these studies predict a $^2\Pi_g$ ground state and assign the IR band as the transition to $^2\Sigma_g^+$. Deeth assigns the Red band to the $^2\Delta_g \longleftarrow {}^2\Pi_g$ transition whilst Rogemond *et al.* describe this band as charge transfer in origin with the ligand-field transition lying at even higher energies. Deeth performed CLF calculations using the assignment of Bauschlicher and Roos and that suggested by the LDF-STO. These calculations and the assignment of the spectrum are discussed further below.

Computational Details

Density functional theory calculations are becoming an increasingly popular method of studying the properties of transition-metal compounds.[29–32] All DFT calculations were performed here using the DEFT code written by St-Amant[33] in the LCGTO framework. Three types of calculation have been completed, differing in the treatment of the exchange and correlation interactions. The first, labelled VWN, used the Vosko–Wilk–Nusair local spin density (LSD) approximation of the exchange-correlation potential.[34] The second, labelled BP, corrects the LSD expression using the Becke[35] non-local functional for exchange and the Perdew[36] non-local functional for correlation. In the third approach, labelled, MIX, the non-local corrections are added perturbatively to the energy and energy gradients of the self-consistent local density. Any changes in the density due to the non-local corrections are neglected in these 'mix' calculations.

The Gaussian basis sets (GTOs) and the auxiliary basis sets needed for the Coulomb and exchange potential were optimized specifically for LSD calculations by Godbout *et al.*[37] For nickel, one GTO set of double-ζ quality was used with two contraction patterns, (63321/531*/41+) and (63321/5211*/41+) (using Huzinaga's notation).[38] It contains one d-diffuse and one p-polarization function. For chlorine, a double-ζ basis set with two contraction patterns, (6321/521/1*) and (7321/621/1*), and a triple-ζ basis set with the contraction pattern (73111/6111/1*) were used. These sets both contain a d-polarization function. Calculations for each of the three approaches (VWN, BP and MIX) described above have been performed with each of the six possible combinations of basis functions. All calculations were performed in an all (62)-electron treatment. Vibrational frequencies were calculated by finite differentiation of analytic first derivatives. The symmetric stretch, the bending mode and the antisymmetric stretch are denoted ν_1, ν_2 and ν_3 respectively.

The CLF model of Gerloch and Woolley[39,40] has been used successfully for many years to model the ligand-field properties of transition-metal complexes. The quantum-mechanical basis of ligand-field theory and the chemical significance of CLF parameters has recently been reviewed.[41] CLF calculations were performed on $NiCl_2$ and $CuCl_2$ using the CAMMAG 4 suite of programs.[42] The CLF calculations used the linear geometries predicted by the DFT treatments for $NiCl_2$ and by the calculations of Rogemond *et al.*[3] for $CuCl_2$. The CLF parameters e_σ(Cl) and e_π(Cl) were used for the σ and π interactions between the transition metal and chlorine. The interpretation of e_σ(Cl) is discussed more fully below. The 'central' Racah parameters *B* and *C* for interelectron repulsion and ζ for spin–orbit coupling were also required for the analysis of $NiCl_2$ using the full d^8 basis of spin triplet and spin singlets. Spin–orbit coupling was included in the $CuCl_2$ calculations.

Results and Discussion

$NiCl_2$

The DFT calculations on $NiCl_2$ using the three approaches described above and the six combinations of basis sets all predict a linear molecule with a $^3\Sigma_g^-$ ground state. Table 1 lists the calculated Ni–Cl bond length and vibrational frequencies for the three levels of theory obtained using the less contracted nickel basis set and the triple-ζ set for chlorine. The calculations for the other combinations of basis sets are not presented in the interests of brevity. The Ni–Cl bond length is found to be considerably more sensitive to the more or less contracted nature of the nickel p functions than to the quality of the chlorine basis set. This result was also observed by Rogemond *et al.*[3] The same trend in the quality of the calculations (as measured by the vibrational frequencies) for the three approaches shown in Table 1 is repeated for the other basis set combinations. The non-local corrections in each case lead to a reduction of the vibrational frequencies. The best results for this open-shell system are found using the Vosko–Wilk–Nusair LSD approximation of the exchange-correlation potential, the less-contracted basis set for nickel and the triple-ζ basis set for chlorine. The Kohn–Sham eigenvalue diagram for this calculation is shown in Fig. 1. The degree of mixing is similar to that found by Rogemond *et al.*[3] in their analogous calculation on $CuCl_2$. The nickel d functions are mixed to a slightly greater extent than those of copper. This is consistent with the greater

Table 1 Calculated and experimentally determined properties of the ground state of $NiCl_2$*

	Geometry		Vibrational frequencies		
	Bond angle/°	Bond length/Å	ν_1	ν_2	ν_3
Calculated VWN	180	2.050	354	70	538
BP	180	2.060	296	110	459
MIX	180	2.071	287	115	445
Experiment (*a*)	180 ± 4	2.056			
(*b*)	—		≈360	87.1	
(*c*)	—		357	88.5	513
(*d*)	—			85	521
(*e*)	—				505/515
(*f*)	Linear	2.056			
(*g*)	≈161				521

* The calculated frequencies and the experimental values are all for the $^{58}Ni^{35}Cl_2$ isotope. The experimental values are from (*a*) analysis of the bond at 460 nm at rotational resolution,[13] (*b*) analysis of this band at vibrational resolution,[11,12] (*c*) the dispersed fluoresence spectrum,[43] (*d*) the IR spectrum in an argon matrix,[19,44] (*e*) the gas-phase IR spectrum,[45,46] (*f*) electron diffraction[47] (also predicted to be linear from electric deflection studies[48]) and (*g*) the IR spectrum in an argon matrix[5] (the isotope analysis has been questioned by Beattie *et al.*[6]).

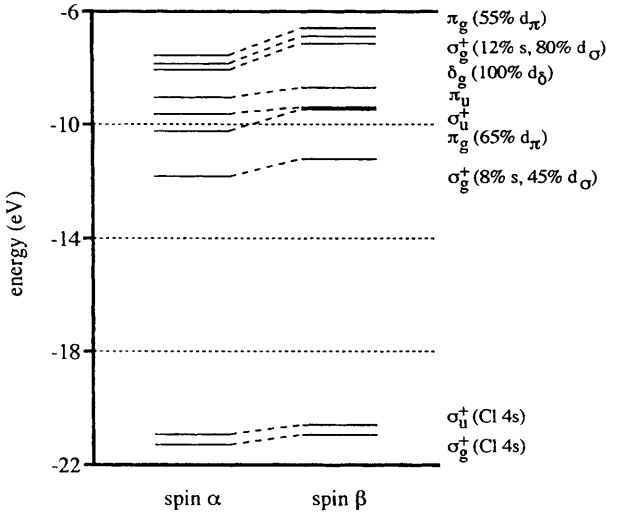

Fig. 1 Kohn-Sham eigenvalue diagram for the $^3\Sigma_g^-$ ground state of $NiCl_2$. The metal d- and s-orbital character is given as a percentage. eV ≈ 1.60 × 10^{-19} J

radial extension of the nickel orbitals due to the lower effective nuclear charge. Starting from the ionic extreme of a $Ni^{2+}2Cl^-$ system, the relative σ-to-π charge donation by the chloride ions is roughly in the ratio 2:1. The lowest-lying excited triplet states were also calculated. The lowest-lying $^3\Pi_g$ state, deriving from a $\delta_g{}^4\sigma_g{}^{+1}\pi_g{}^3$ configuration, was found to lie *ca.* 3000 cm^{-1} above the ground state. The $^3\Phi_g$ state, deriving from a $\delta_g{}^4\sigma_g{}^{+1}\pi_g{}^3$ configuration, lay *ca.* 4000 cm^{-1} above the ground state. The DFT calculations suggest that there are no low-lying excited states so that the character of the ground state is likely to be relatively unaffected by mixing due to spin–orbit coupling.

The recent experimental results outlined above and the DFT calculations presented here all concur that $NiCl_2$ has a $^3\Sigma_g^-$ ground state. Such a state can only arise from a $\delta_g{}^4\sigma_g{}^{+2}\pi_g{}^2$ or $\pi_g{}^4\sigma_g{}^{+2}\delta_g{}^2$ configuration. Using CLF calculations, it is possible to explore the parameter values that would be required to generate such configurations and the observed ground state for linear, d^8 MX_2 molecules. A $^3\Sigma_g^-$ ground state derived from a $\pi_g{}^4\sigma_g{}^{+2}\delta_g{}^2$ configuration requires negative values for both e_π and e_σ and this is discounted. The $\delta_g{}^4\sigma_g{}^{+2}\pi_g{}^2$ configuration requires the antibonding shift of the d_σ function to be less than that of the d_π. Such a circumstance was rejected by Lever and Hollebone[14] in their considerations of the possible ground state of this system, because it was taken to imply greater π than σ-donation by the ligand X. The DFT calculations on $NiCl_2$ suggest the familiar σ > π donation from the chloride ions, a result also found in the DFT analysis of Deeth[2] on $CuCl_2$.

The lower than expected energy of the d_σ orbital is reminiscent of the situation found in planar metal(II) complexes[49,50] where the d_{z^2} orbital (with the *z* axis taken perpendicular to the molecular plane) is shifted downward in energy by ≈6000 cm^{-1} for $[CuCl_4]^{2-}$ and ≈12 000 cm^{-1} for $[PtCl_4]^{2-}$, a substantial effect. The angular overlap model (AOM) accounts for this by enlarging the pure d-orbital basis to include s functions. In the D_{4h} point group appropriate for planar MX_4 systems, both the metal d_{z^2} and s orbitals transform as the totally symmetric representation, a_{1g}. The mixing of these two functions, represented by the additional AOM parameter e_{ds}, then causes the observed stabilization of the d_{z^2} orbital. Smith[49] also used this idea to interpret the spectrum of linear $CuCl_2$, since in the $D_{\infty h}$ point group the metal d_σ and s orbitals both transform as σ_g^+.

In the CLF model, the apparently anomalous energy of the d_{z^2} orbital in planar MX_4 and related systems is accounted for without an *ad hoc* extension of the ligand-field basis by consideration of the potential in the empty or void 'cell' regions above and below the molecular plane.[39-41] This idea may be extended to linear molecules. In the CLF model the total ligand-field potential is divided into local regions or cells. The parameters, e_λ, are the energy shifts of the local d orbitals of λ symmetry by the local ligand-field potential. They are dominated by the so-called 'dynamic' contribution[39,40] (1) and

$$e_\lambda^c \approx \sum_\chi \frac{\langle d_\lambda^c|\mathscr{H}^{(1)}|\chi_\lambda^c\rangle\langle\chi_\lambda^{(c)}|\mathscr{H}^{(1)}|d_\lambda^{(c)}\rangle}{\varepsilon_d - \tilde{\varepsilon}_\lambda} \quad (1)$$

since by definition, $e_\lambda^c = \langle d_\lambda^c|v^c|d_\lambda^c\rangle$ the local ligand-field potential, v^c, is given by equation (2); λ labels the local

$$v^c \approx \sum_\chi \frac{\mathscr{H}^{(1)}|\chi_\lambda^{(c)}\rangle\langle\chi_\lambda^{(c)}|\mathscr{H}^{(1)}}{\varepsilon_{LF} - \tilde{\varepsilon}_\lambda} \quad (2)$$

functions as of σ or π symmetry and all terms with a 'c' superscript refer to locally defined (cellular) quantities. The χ functions, with mean energy $\tilde{\varepsilon}_\lambda$, are built from all the non-d functions in the molecule. The terms in the summation likely to be significant will be those where the χ functions are spatially and energetically close to the d orbitals. These functions are the bonding and low-lying antibonding orbitals in the molecule. The global operator $\mathscr{H}^{(1)}$ is the aspherical part of the potential-energy operator *V*, where *V* is a function of the total molecular electron density minus that of the d electrons. A non-zero local potential requires a non-zero $\mathscr{H}^{(1)}$ and χ_λ^c in the local region c.

The total (non-d) electron density in a MX_2 molecule of $D_{\infty h}$ symmetry will be cylindrically symmetric about the molecular axis. The aspherical part of this density and hence the aspherical

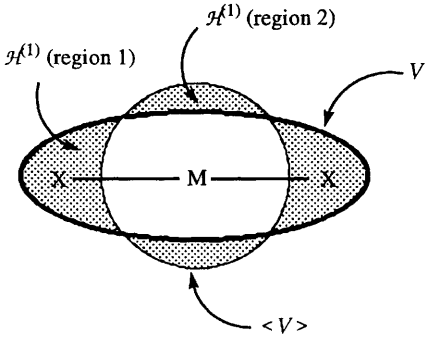

Fig. 2 A cross-section containing the molecular axis of the potential in an MX_2 molecule of $D_{\infty h}$ symmetry due to the non-d-electron density. The area within the heavily shaded line represents the total potential (V). The circular area contained within the lighter line represents the spherical part ($\langle V \rangle$) and the shaded area represents the aspherical part ($\mathcal{H}^{(1)}$) of this potential

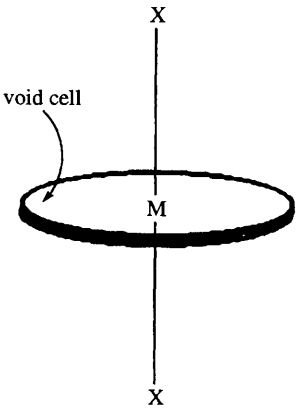

Fig. 3 The void cell required properly to account for the downward shift of d_σ in linear MX_2 molecules

part of the potential, $\mathcal{H}^{(1)}$, will be non-zero in regions near the ligand (region 1) and in a cylindrically symmetric band around the metal (region 2). A cross-section of the potential containing the molecular axis is represented in Fig. 2. The σ_g^+ ligand-group orbital in this molecule overlaps with the metal s orbital to form a bonding and an antibonding orbital. The former is full, is dominated by ligand-based functions and is maximal in the same part of space as region 1 of $\mathcal{H}^{(1)}$. For the cell containing the ligand this leads to non-zero e_σ parameters, denoted e_σ'(Cl) here for reasons discussed below. The antibonding orbital is empty and resembles the metal s function. It is maximum in the same part of space as region 2 of $\mathcal{H}^{(1)}$. The local ligand-field potential, v^c in equation (2), for the unco-ordinated ('void') region perpendicular to the molecular axis is thus non-zero. The energy of the antibonding orbital is greater than that of the mean d orbitals and so the denominator in equation (1) is negative. Since the numerator is necessarily positive, this causes a downward shift in the energy of any d orbital with the same symmetry.

In planar MX_4 systems the equivalent arguments[39,41] lead to $\mathcal{H}^{(1)}$ being non-zero in localized regions above and below the molecular plane and it is technically sensible to locate void cells in these regions to define local axis frames. In the present system the important region of $\mathcal{H}^{(1)}$ is cylindrically symmetric and cannot be localized into separate cells. The void cell must be taken as the cylindrically symmetric region perpendicular to the molecular axis shown in Fig. 3. The local *pseudo*-symmetry for this cell is $D_{\infty h}$. The only d orbital with the same symmetry as that as the part of the σ_g^+ antibonding orbital in this cell is the global d_σ orbital. The antibonding orbitals formed between the remaining ligand and metal (non-d) functions all have local *ungerade* symmetry and cannot interact with the d functions. Using $2e_\sigma$(void) to represent the interaction of the d_σ orbital with the antibonding orbital, the d-orbital energies are given by equations (3a)–(3c). As both e_σ(Cl) and e_σ(void) only affect the

$$\varepsilon(d_\sigma) = 2e_\sigma'(\text{Cl}) + 2e_\sigma(\text{void}) \quad (3a)$$

$$\varepsilon(d_\pi) = 2e_\pi(\text{Cl}) \quad (3b)$$

$$\varepsilon(d_\delta) = 0 \quad (3c)$$

d_σ orbital, it is impossible to separate their effects and it is more appropriate to define a composite parameter, equation (4), and

$$e_\sigma(\text{Cl}) = e_\sigma'(\text{Cl}) + e_\sigma(\text{void}) \quad (4)$$

equation (3b) then simplifies to (3d). It is these parameter

$$\varepsilon(d_\sigma) = 2e_\sigma(\text{Cl}) \quad (3d)$$

definitions that are used in the present analysis. The parameter e_σ(Cl) is a sum of a positive and a negative term. As noted above, the void effect is known to be important in planar four-co-ordinate systems. The magnitude of e_σ(Cl) in the present linear system is similarly expected to be reduced from 'normal' e_σ values and its sign could, in principle, be either positive or negative. The CLF parameters derived from the analysis of the spectra of $NiCl_2$ and $CuCl_2$ should be interpreted on this basis. The only CLF parameters that can be obtained from a ligand-field analysis are e_σ(Cl) and e_π(Cl). The parametrization scheme is thus indistinguishable from that used by Lever and Hollebone[14] but the interpretation of the results is quite different. In their study of the spectra of metal dihalides, they rejected ground states and spectral assignments that required the apparently counter-intuitive result that $e_\sigma(\text{Cl}) < e_\pi(\text{Cl})$. In view of the discussion above and, in particular, the composite nature of e_σ(Cl), a $^3\Sigma_g^-$ ground state for $NiCl_2$ and a $^2\Pi_g$ ground state for $CuCl_2$ cannot be so easily discounted.

Deeth[2] attempted to model the void cell described above by locating eight 'dummy' ligands at 45° intervals in the plane perpendicular to the molecular axis containing the metal. Although, as noted above, it is technically reasonable to model the void regions using localized cells because of the cyclindrically symmetric nature of $\mathcal{H}^{(1)}$ in the present system, this method of modelling is inappropriate. Owing to the disposition of the 'dummy' ligands, the global symmetry is reduced to D_{8h}. In this point group the 'd_δ' orbitals are also affected by the ligand field. This modelling leads to a downward shift of each of these orbitals. In reality, however, there are no (low-lying) bonding or antibonding orbitals of δ symmetry to cause such a shift. The result of modelling the void interaction in this way is to introduce a negative e_δ contribution.

It is worthwhile at this point to underline the circumstances in which the 'void cell effect' may usefully be employed. The CLF model is based on a decomposition of the total (or global) ligand-field potential. The global symmetry of the complex cannot be neglected or ignored. This problem may be illustrated by reference to complexes with strict and distorted octahedral symmetry.

For a ML_6 complex of strict O_h symmetry the six ligand σ functions span a_{1g}, e_g and t_{1u}. The a_{1g} and t_{1u} combinations may overlap respectively with the metal s orbital and p orbitals generating bonding and antibonding orbitals. In O_h symmetry, however, none of these provides a ligand-field source. The global integrals $\langle d|\mathcal{H}^{(1)}|\chi_\lambda\rangle$, where λ is a_{1g} or t_{1u}, vanish as the d orbitals transform as e_g or t_{2g}. Only the e_g combination of the ligand σ functions can provide a source for the e_g d orbitals. Similarly, only the t_{2g} combination of ligand π functions can provide a source for the metal t_{2g} d orbitals.

Now consider three distortions of this octahedral complex. In each case to simplify the picture the ligands are assumed to be π-

Table 2 Calculated and observed transition energies (in cm^{-1}) in the ligand-field spectrum of $NiCl_2$

State*	Strong-field configuration*	Ω	Calculated	Observed[7–9]
$^1\Sigma_g^+$ (S)	$\delta_g^2\sigma_g^2\pi_g^4$	0+	47 689	
$^1\Gamma_g$ (G)	$\delta_g^2\sigma_g^2\pi_g^4$	4	28 600	
$^1\Delta_g$ (G)	$\delta_g^3\sigma_g^1\pi_g^4$	2	22 058	
$^3\Sigma_g^-$ (P)	$\delta_g^2\sigma_g^2\pi_g^4$	0+	21 769	21 700
		1	21 703	
$^1\varphi_g$ (G)	$\delta_g^3\sigma_g^2\pi_g^3$	3	21 370	
$^1\Sigma_g^+$ (G)	$\delta_g^4\sigma_g^2\pi_g^4$	0+	18 732	18 000
$^1\Pi_g$ (G)	$\delta_g^3\sigma_g^2\pi_g^3$	1	18 630	
$^1\Sigma_g^+$ (D)	$\delta_g^4\sigma_g^1\pi_g^3$	0+	16 618	16 000
$^1\Pi_g$ (D)	$\delta_g^4\sigma_g^1\pi_g^3$	1	15 455	
$^3\Pi_g$ (P)	$\delta_g^3\sigma_g^2\pi_g^3$	0−	13 698	14 000
		0+	13 523	
		2	13 286	
		1	13 127	13 000
$^1\Delta_g$ (D)	$\delta_g^4\sigma_g^2\pi_g^2$	1	11 732	11 727
$^3\Delta_g$ (F)	$\delta_g^3\sigma_g^1\pi_g^4$	1	9 617	10 000
		2	9 114	
		3	8 463	
$^3\Phi_g$ (F)	$\delta_g^3\sigma_g^2\pi_g^3$	2	7 074	4 000–6 000
		3	6 193	
		4	5 363	
$^3\Pi_g$ (F)	$\delta_g^4\sigma_g^1\pi_g^3$	0+	4 453	
		0−	4 256	
		1	3 973	
		2	3 465	
$^3\Sigma_g$ (F)	$\delta_g^4\sigma_g^2\pi_g^2$	1	115	
		0+	0	

* Approximate description.

neutral. If one metal–ligand bond is lengthened slightly along the global z axis the molecular symmetry is lowered to C_{4v}. The a_1 molecular orbital can now act as a ligand-field source but only for the d_{z^2} orbital since this uniquely transforms as the totally symmetric representation. The antibonding orbital formed from the a_1 combination of ligand σ functions and the metal s orbital may similarly contribute to the local e_σ value for the lengthened bond. The resulting e_σ value is the sum of these two contributions, as in equation (1). If the distortion is increased the contribution to the local e_σ parameter from the bonding a_1 orbital steadily decreases. It reduces to zero in the limit of a vanishing ligand. The character of the antibonding a_1 orbital becomes more metal s-like as the distortion increases so that the local part of the aspherical potential $\mathscr{H}^{(1)}$ and the antibonding orbital maximize closer to the local d_σ orbital. The result is that the contribution from the antibonding a_1 orbital to the local e_σ parameter increases in magnitude. The denominator is negative for this term in the summation in equation (1) and an increasingly negative contribution to the local e_σ parameter results. The ligand-field strength of the bond decreases from its value in the octahedral complex through zero to a negative value as the ligand is steadily removed.

If the octahedral complex is distorted by steadily removing two *trans* ligands along the z axis the global symmetry is lowered to D_{4h}. A similar picture emerges[39,41] as that outlined for the C_{4v} complex. The global bonding and antibonding a_{1g} orbitals can act as a ligand-field source only for the d_{z^2} orbital. It is then appropriate to model the effect of the antibonding a_{1g} orbital using two sources or 'voids' located on the z axis. The ligand-field strength of the *trans* bonds decrease from their values in the octahedral complex through zero to negative values as the ligands are steadily removed.

Finally, four equatorial ligands can simultaneously be removed along the x and y axes of the octahedron. The linear compounds that form the subject of this paper may be regarded as the limiting case of such a distortion. This distortion also lowers the global symmetry to D_{4h}. The degeneracy of the e_g ligand combination in the octahedron is split by the distortion into a_{1g} and b_{1g}. The former may act as a ligand-field source for the global d_{z^2} orbital. The latter may act as a source for the global $d_{x^2-y^2}$ orbital. The d_{z^2} orbital is thus perturbed by both the bonding and the increasingly 's'-like antibonding a_{1g} orbitals. The $d_{x^2-y^2}$ orbital is only affected by the b_{1g} bonding combination. As the four ligands are removed their e_σ values decrease smoothly to zero at the limiting case of the linear molecule. There is no antibonding b_{1g} orbital that can affect the global $d_{x^2-y^2}$ orbital so that there is no negative contribution to the e_σ(equatorial) parameters. The negative contribution to the e_σ(axial) values may be modelled using the cylindrical void cell described above. The expression of the global ligand field as a superposition of locally defined contributions must be carried out with due regard to the global molecular symmetry.

The parametrization scheme described above for a linear MX_2 molecule may also be used for a bent system. In C_{2v} symmetry both the global d_{z^2} and $d_{x^2-y^2}$ orbitals transform as a_1. The bonding and antibonding functions of the same symmetry act as ligand-field sources for both of these orbitals. The void cell will no longer be cylindrically symmetric and its shape will be dependent on the extent of distortion. As for the linear systems, the only parameters that can be determined are e_σ(X) and e_π(X) with the former a composite of the ligand and void-cell contributions, as in equation (4). The resulting shifts and the relative energies of the global d_{z^2} and $d_{x^2-y^2}$ orbitals are then dependent on the size of the contributions to e_σ(X) and by the angular geometry.

Using the correct interpretation of the CLF parameters, a $^3\Sigma_g^-$ ground state is obtained from positive e_σ and e_π parameters and with $e_\pi > e_\sigma$. The CLF analysis yields an excellent fit to the observed transition energies. Table 2 lists the observed and calculated transition energies and their assignments. The band at 21 700 cm^{-1} has received considerable experimental attention, as reviewed above. It is assigned as $^3\Sigma_g^-$ (P) ⟵ $^3\Sigma\Omega_g^-$ (F) in agreement with the suggestion of Ashworth *et al.*[12] Fig. 4 shows the calculated energy-level diagram for the two states involved in this transition and a comparison with the fine structure observed in the spectral band. The agreement between the CLF calculation and the observed splitting is reasonable and strongly supports this assignment. The sharp band at *ca.* 11 700 cm^{-1} is assigned to the transition $^1\Delta_g$ (D) ⟵ $^3\Sigma_g^-$(F). Both of these states correlate with the same strong-field configuration, $\delta_g^4\sigma^{+2}{}_g\pi_g^2$. The equilibrium bond length in the two states is therefore likely to be very similar and so rationalizes the sharp transition that is observed.

The CLF parameter values obtained differ markedly with those of Lever and Hollebone[14] in their analysis of this system, as shown in Table 3. These differences result from the different ground states and assignments used in the two analyses. In the calculations of Lever and Hollebone the ground state is $^3\Pi_g$ (F) and is found to be 879 cm^{-1} below the $^3\Sigma_g^-$ (F) state. In the calculations presented here the ground state is $^3\Sigma_g^-$ (F) and is found to be *ca.* 3500 cm^{-1} below the $^3\Pi_g$ (F) state.

It is interesting to compare the e_λ values obtained for $NiCl_2$ with those for $[NiCl_4]^{2-}$. The geometry of the latter closely approaches T_d symmetry and the spectrum can be fitted[51] using the single cubic-field splitting parameter, Δ_{tet}. It has been empirically observed[53] that the trace, Σ, of the global ligand-field matrix is approximately constant (at ≈22 000 cm^{-1}) for a wide range of complexes of Co^{II}, Ni^{II} and Cu^{II} with different co-ordination numbers, geometries and ligand types. The trace is equal to the sum of all e_λ parameters for the whole complex. Using this concept of parameter transferability yields the CLF parameter values for $[NiCl_4]^{2-}$ listed in Table 3. The most immediately obvious difference is the large increase in e_π(Cl) for $NiCl_2$ relative to $[NiCl_4]^{2-}$. This suggests an increase in the π donation by the chloride ligands and presumably reflects the trend of the nickel cation to achieve electroneutrality in this low-co-ordination number system. The ratio e_π(Cl):e_σ(Cl) is

Table 3 The CLF parameter values (in cm^{-1}) for $NiCl_2$, $[NiCl_4]^{2-}$, $CuCl_2$ (assignments I and II as defined in the text) and planar $[CuCl_4]^{2-}$

Compound	e_σ(Cl)	e_π(Cl)	e_π(Cl)/e_σ(Cl)	Σ	B	C	ζ
$NiCl_2$ [a]	2309	3621	1.57	19 102	614	3808	650
$NiCl_2$ [b]	4798	3098	0.65	21 988	725	5436	—
$[NiCl_4]^{2-}$ [c]	3800	900	0.24	22 400	780	—	550
$CuCl_2$ (I)	4680	8950	1.91	45 160	—	—	700 [d]
$CuCl_2$ (II)	3690	3870	1.05	22 860	—	—	700 [d]
$[CuCl_4]^{2-}$ [e]	5400	900	0.17	22 950	—	—	700 [d]

[a] This work. [b] From Lever and Hollebone.[14] [c] From ref. 51. [d] Held fixed. [e] From ref. 52 for the compound *N*-methylphenethylammonium tetrachlorocuprate. The analysis also included e_σ(void) = 2925 cm^{-1}.

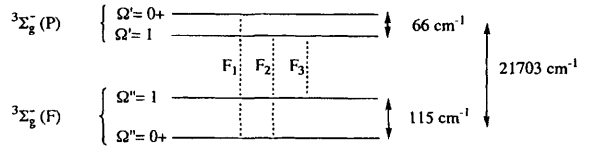

Fig. 4 Calculated energy-level diagram for the states involved in the $^3\Sigma_g^-$ (P) ⟵ $^3\Sigma\Omega_g^-$ (F) transition assigned to the 21 700 cm^{-1} (470 nm) band in the spectrum of $NiCl_2$. The components labelled F_1, F_2 and F_3 have been experimentally observed in the high-resolution spectrum[11] with splittings of 95.9 ($F_1 - F_2$) and 149.1 cm^{-1} ($F_2 - F_3$)

≈1.6:1. The small value for e_σ(Cl) must be interpreted, as detailed above, as the result of the sum of a positive [e_σ'(Cl)] and a negative [e_σ(void)] term. If for illustrative purposes the downward shift in the energy of d_σ is taken to be similar to the ≈6000 cm^{-1} stabilization of d_{z^2} observed[49] in planar $[CuCl_4]^{2-}$, e_σ'(Cl) ≈ 5300 cm^{-1}. The ratio e_π(Cl):e_σ'(Cl) is ≈0.7:1, consistent with chloride acting as a better σ than π donor in $NiCl_2$, in line with the DFT results and chemical expectations. Such a value for e_σ'(Cl) suggests that there is also an increase in the σ donation by the chloride ligand in the low-co-ordination number system. The probably larger increase in the π basicity may be a reflection of the greater sensitivity of π overlap to internuclear separation (the bond length for $NiCl_2$ is ≈2.05 Å and that for $[NiCl_4]^{2+}$ is *ca.* 2.27 Å)[54] and the lower steric repulsion by the d electrons to π bonding because of the presence of two holes in the d_π orbitals in the $^3\Sigma_g^-$ ground state. The value of the ligand-field trace, Σ, found for $NiCl_2$ is slightly lower than that for $[NiCl_4]^{2+}$ but not markedly so.

$CuCl_2$

In Deeth's CLF analysis of $CuCl_2$ two assignments of the absorption spectrum were considered. The first assignment (I) uses Deeth's DFT calculations and assigns the IR band (*ca.* 9000 cm^{-1}) to the $^2\Sigma_g^+$ ⟵ $^2\Pi_g$ transition and the Red band (*ca.* 19 000 cm^{-1}) to the $^2\Delta_g$ ⟵ $^2\Pi_g$ transition. The second assignment (II) uses the results of Bauschlicher and Roos[1] with the $^2\Sigma_g^+$ ⟵ $^2\Pi_g$ transition lying outside the experimental spectral window at *ca.* 1500 cm^{-1} and the $^2\Delta_g$ ⟵ $^2\Pi_g$ transition assigned to the IR band. The CLF calculations employed the incorrect modelling of the void interaction as described above and are ignored. These d–d transitions are only allowed by the electric-dipole mechanism through vibronic coupling with the *ungerade* bending (ν_2) and antisymmetric stretch (ν_3) vibrational modes. The only transitions from the $^2\Pi_g$ ($\Omega = \frac{1}{2}$) ground state that are allowed by this mechanism are to the $^2\Pi_g$ ($\Omega = \frac{3}{2}$) (by ν_3), $^2\Sigma_g^+$($\Omega = \frac{1}{2}$) (by ν_3) and $^2\Delta_g$ ($\Omega = \frac{3}{2}$) (by ν_2) excited states.† The transition to $^2\Delta_g$ ($\Omega = \frac{5}{2}$) is forbidden. The spectral band assigned to the $^2\Delta_g$ ⟵ $^2\Pi_g$ transition in assignments I and II is taken here as the transition to the $\Omega' = \frac{3}{2}$ component of $^2\Delta_g$. Table 3 lists the CLF parameters required for the two assignments and those obtained[55] for planar $[CuCl_4]^{2-}$.

The results of the CLF analysis suggest that assignment II is more likely. The value of e_π(Cl) for assignment I represents a ten-fold increase on the value obtained for $[CuCl_4]^{2-}$ and a two-fold increase on the value for $NiCl_2$. The bond length for $CuCl_2$ is calculated to be 2.065 Å by Deeth[2] and 2.047 Å by Rogemond *et al.*[3] These values are very close to the bond length for $NiCl_2$, shown in Table 1, and suggest that such a large change in π donation between the two dihalides is unlikely. The small increase in e_π found for assignment I, however, seems entirely feasible in view of the extra electron in the d_π orbitals but the higher effective nuclear charge for Cu^{2+}. The values for e_σ(Cl) are more difficult to compare due to the summation in equation (4). If the stabilization of d_σ is again taken to be ≈6000 cm^{-1} the values of e_σ'(Cl) are calculated to be approximately 7700 and 6700 cm^{-1} for assignments I and II respectively. Both are larger than the value for $NiCl_2$; a similar trend is observed for the nominally tetrahedral $[NiCl_4]^{2-}$ and $[CuCl_4]^{2-}$ ions.[51,53] Neither value for e_σ'(Cl) can be ruled out in isolation, however. On the other hand, the value of the ligand-field trace, Σ, for assignment II is very close to the value found for the $[CuCl_4]^{2-}$ ion in a variety of systems.[52,53] The value for assignment I though is roughly twice as large as that deemed 'normal' and, indeed, that obtained for $NiCl_2$. Altogether, assignment I appears unsatisfactory.

Conclusion

The LCGTO-DFT calculations on $NiCl_2$ predict that the molecule is linear with the unexpected $^3\Sigma_g^-$ ground state recently suggested by experiment. The optimum bond length and vibrational frequencies also agree very well with experiment. A CLF analysis of the spectrum yields parameters that are consistent with the DFT description of the bonding. The calculations suggest that the σ and π basicity of the chloride ions are enhanced compared to systems with higher co-ordination numbers as the metal tries to maintain its electroneutrality.

The reanalysis reported here strongly suggests an assignment of the spectrum of $CuCl_2$ consistent with the CPF-HF calculations of Bauschlicher and Roos[1] and the calculations on $NiCl_2$. The description of the bonding provided by the CLF analysis using this assignment suggests that the bonding in $NiCl_2$ and $CuCl_2$ is quite similar.

Analyses of systems such as this require a proper account of the interaction between the d_σ orbital and the σ_g^+ antibonding orbital of mostly metal s-orbital character. It might appear that the disagreement with Deeth's approach to modelling the void interaction using eight 'dummy' ligands is simply a matter of taste. It is more than a technical objection on the basis of symmetry. Deeth's treatment led to e_σ(Cl) < e_π(Cl), a result which appeared chemically surprising and totally out of line with other CLF/AOM analyses. The treatment described here,

† Extensive experimental and theoretical studies[55] on $[CuCl_4]^{2-}$ suggest that bending modes are much more efficient generators of intensity. The higher temperatures used to record the spectrum of the present system lead to a large amplitude for the soft bending mode, ν_2, amplifying its ability to generate intensity. The relative intensity of the $^2\Sigma_g^+$ ⟵ $^2\Pi_g$ transition might then be quite small and this could account for the possible absence of this transition in low-resolution spectra.

however, with the void treated properly, leads naturally to the result $e_\sigma'(\mathrm{Cl}) > e_\pi(\mathrm{Cl})$. The actual value of this ratio cannot be obtained and it is important to note that CLF/AOM parameters must always be interpreted in this way with due regard for the global molecular symmetry. Nothing in the analyses of $NiCl_2$ and $CuCl_2$ appears surprising.

Acknowledgements

The author would like to thank Dr. Malcolm Gerloch for helpful discussions and for the use of the CAMMAG 4 program suite and Dr. Alain St-Amant of the University of Ottawa for making the DEFT code publicly available.

References

1 C. W. Bauschlicher, jun., and B. O. Roos, *J. Chem. Phys.*, 1989, **91**, 4785.
2 R. J. Deeth, *J. Chem. Soc., Dalton Trans.*, 1993, 1061.
3 F. Rogemond, H. Chermette and D. R. Salahub, *Chem. Phys. Lett.*, 1994, **219**, 228.
4 I. R. Beattie, P. J. Jones and N. A. Young, *Mol. Phys.*, 1991, **72**, 1309.
5 D. W. Green, D. P. McDermott and A. J. Bergman, *J. Mol. Spectrosc.*, 1983, **98**, 111.
6 I. R. Beattie, P. J. Jones and N. A. Young, *Chem. Phys. Lett.*, 1991, **177**, 579.
7 J. T. Hougen, G. E. Leroi and T. C. James, *J. Chem. Phys.*, 1961, **34**, 1670.
8 C. W. DeKock and D. M. Gruen, *J. Chem. Phys.*, 1966, **44**, 4387.
9 C. W. DeKock and D. M. Gruen, *J. Chem. Phys.*, 1967, **46**, 1096.
10 L. R. Zink, F. J. Grieman, J. M. Brown, T. R. Gilson and I. R. Beattie, *J. Mol. Spectrosc.*, 1991, **146**, 225.
11 F. J. Grieman, S. H. Ashworth, J. M. Brown and I. R. Beattie, *J. Chem. Phys.*, 1990, **92**, 6365.
12 S. H. Ashworth, F. J. Grieman and J. M. Brown, *Chem. Phys. Lett.*, 1990, **175**, 660.
13 S. H. Ashworth, F. J. Grieman, J. M. Brown, P. J. Jones and I. R. Beattie, *J. Am. Chem. Soc.*, 1993, **115**, 2978.
14 A. B. P. Lever and B. R. Hollebone, *Inorg. Chem.*, 1972, **11**, 2183.
15 E. P. F. Lee, A. W. Potts, M. Dovan, I. H. Miller, J. J. Delaney and R. W. Hawksworth, *J. Chem. Soc., Faraday Trans. 2*, 1980, 508.
16 A. W. Potts, D. Law and E. P. F. Lee, *J. Chem. Soc., Faraday Trans. 2*, 1981, 797.
17 D. W. Smith, *Inorg. Chim. Acta*, 1971, **5**, 231.
18 J. Berkowitz, D. G. Streets and A. Garritz, *J. Chem. Phys.*, 1979, **70**, 1305.
19 M. E. Jacox and D. E. Milligan, *J. Chem. Phys.*, 1969, **51**, 4143.
20 T. K. Ha and M. T. Nguyen, *Z. Naturforsch., Teil A*, 1984, **39**, 175.
21 P. Correa De Mello, M. Hehenberger, S. Larsson and M. C. Zerner, *J. Am. Chem. Soc.*, 1980, **102**, 1278.
22 M. C. Zerner, in *Metal–ligand interactions: from atoms to molecules, to surfaces*, eds. D. R. Salahub and N. Russo, Kluwer, Dordrecht, 1992.
23 T. Tokuda, N. Fujii, S. Yoshuda, K. Shimuza and I. Tanaka, *Chem. Phys. Lett.*, 1990, **174**, 385.
24 A. J. Bouvier, R. Bacis, J. Bonnet, S. Churasy, P. Crozet, B. Erba, J. B. Koffend, J. Lamarre, M. Lamrini, D. Pigache and A. J. Ross, *Chem. Phys. Lett.*, 1991, **184**, 133.
25 H. P. Yang, Y. Qin, Q. N. Yuan, X. B. Xie, Q. Zhuang and C. H. Zhuang, *Chem. Phys. Lett.*, 1992, **191**, 130.
26 T. Tokuda and N. Fujii, *J. Phys. Chem.*, 1992, **96**, 6504.
27 A. J. Ross, R. Bacis, A. J. Bouvier, S. Churassy, J.-C. Coste, P. Crozet amd I. Russier, *J. Mol. Spectrosc.*, 1993, **158**, 27.
28 P. Crozet, A. J. Ross, R. Bacis, M. P. Barnes and J. M. Barnes, *J. Mol. Spectrosc.*, 1995, **43**, 172.
29 *Local Density Approximations in Quantum Chemistry and Solid-state Physics*, eds. J. P. Dahl and J. Avery, Plenum, New York, 1989.
30 R. G. Parr and W. Yang, *Density-functional Theory of Atoms and Molecules*, Oxford University Press, Oxford, 1989.
31 *Density Functional Methods in Chemistry*, eds. J. K. Labanowski and J. W. Andelm, Springer, New York, 1991.
32 T. Ziegler, *Chem. Rev.*, 1991, **91**, 651.
33 DEFT, a FORTRAN program, A. St-Amant, University of Ottawa.
34 S. H. Vosko, L. Wilk and M. Nusair, *Can. J. Phys.*, 1980, **58**, 1200.
35 A. D. Becke, *Phys. Rev. A*, 1988, **38**, 3098.
36 J. P. Perdew, *Phys. Rev. B*, 1986, **33**, 8822.
37 N. Godbout, D. R. Salahub, J. Andzelm and E. Wimmer, *Can. J. Chem.*, 1992, **70**, 1992.
38 *Gaussian Basis Sets for Molecular Calculations*, ed. S. Huzinaga, Elsevier, New York, 1984.
39 M. Gerloch, J. H. Harding and R. G. Woolley, *Struct. Bonding (Berlin)*, 1981, **46**, 1.
40 M. Gerloch, *Magnetism and Ligand-Field Analysis*, Cambridge University Press, Cambridge, 1984.
41 A. J. Bridgeman and M. Gerloch, *Prog. Inorg. Chem.*, in the press.
42 CAMMAG 4, a FORTRAN program, A. R. Dale, M. J. Duer, N. D. Fenton, M. Gerloch and R. F. McMeeking, University of Cambridge, 1996.
43 L. R. Zink, J. M. Brown, T. R. Gilson and I. R. Beattie, *Chem. Phys. Lett.*, 1988, **146**, 501.
44 K. R. Thompson and K. D. Carlson, *J. Chem. Phys.*, 1968, **49**, 4379.
45 S. P. Randall, F. T. Greene and J. L. Margrave, *J. Phys. Chem.*, 1959, **63**, 758.
46 G. E. Leroi, T. C. James, J. T. Hougen and W. Klemperer, *J. Chem. Phys.*, 1962, **36**, 2879.
47 M. Hargittai, N. Y. Subbotina, M. Kolonits and A. G. Gershikov, *J. Chem. Phys.*, 1991, **94**, 7278.
48 A. Büchler, J. L. Stauffer and W. Klemperer, *J. Am. Chem. Soc.*, 1964, **86**, 4544.
49 D. W. Smith, *Inorg. Chim. Acta*, 1977, **22**, 107.
50 A. J. Bridgeman and M. Gerloch, *Mol. Phys.*, 1993, **79**, 1195.
51 C. A. Brown, M. J. Duer, M. Gerloch and R. F. McMeeking, *Mol. Phys.*, 1988, **64**, 793.
52 M. J. Duer, S. J. Essex and M. Gerloch, *Mol. Phys.*, 1993, **79**, 1167.
53 R. J. Deeth and M. Gerloch, *J. Chem. Soc., Dalton Trans.*, 1986, 1531.
54 J. R. Wiesner, R. C. Srivastava, C. H. L. Kennard, M. DiVaira and E. C. Lingafelter, *Acta Crystallogr.*, 1967, **23**, 565.
55 A. J. Bridgeman and M. Gerloch, *Inorg. Chem.*, 1995, **34**, 437.

Received 21*st March* 1996; *Paper* 6/01981A